Hindawi
International Journal of Optics
Volume 2018, Article ID 9452540, 11 pages
https://doi.org/10.1155/2018/9452540

Research Article

On the Creation of Solitons in Amplifying Optical Fibers

Christoph Mahnke, Alexander Hause, and Fedor Mitschke

Institut für Physik, Universität Rostock, 18059 Rostock, Germany

Correspondence should be addressed to Fedor Mitschke; fedor.mitschke@uni-rostock.de

Received 20 December 2017; Accepted 4 February 2018; Published 7 March 2018

Academic Editor: Murugan Senthil Mani Rajan

We treat the creation of solitons in amplifying fibers. Strictly speaking, solitons are objects in an integrable setting while in real-world systems loss and gain break integrability. That case usually has been treated in the perturbation limit of low loss or gain. In a recent approach fiber-optic solitons were described beyond that limit, so that it became possible to specify how and where solitons are eventually destroyed. Here we treat the opposite case: in the presence of gain, new solitons can arise from an initially weak pulse. We find conditions for that to happen for both localized and distributed gain, with no restriction to small gain. By tracing the energy budget we show that even when another soliton is already present and copropagates, a newly created soliton takes its energy from radiation only. Our results may find applications in amplified transmission lines or in fiber lasers.

1. Introduction

Solitons are fascinating objects. They arise from a variety of nonlinear wave equations; here we will concentrate on the Nonlinear Schrödinger Equation (NLSE) and fiber-optic solitons as these represent the only type of solitons that has already seen commercial application [1]. Fiber-optic solitons are light pulses which balance the fiber's dispersion with its nonlinearity such as to stabilize their shape; this makes them eminently suitable as signalling light pulses in optical data transmission. For any other type of soliton a similar interplay of effects produces a similar self-stabilization.

For the NLSE, Zakharov and Shabat found the soliton solution in their ground-breaking paper [2] (called ZS hereafter). This was followed by an equally important paper by Satsuma and Yajima [3] (hereafter, SY) where the pertaining initial-value problem was solved. Both together established the basics of solitons in fibers as they were suggested in [4]; experimentation commenced a few years later [5].

When it comes to real-world settings rather than the idealized context of the integrable NLSE, one has to deal with the impact of power loss on solitons. This issue was treated with perturbation methods by several authors [6–11]. However, such approach requires that the loss be weak and can cover neither strong attenuation coefficients nor long distances with weak coefficients. Moreover, it entirely misses the eventual decay of the soliton. For a long time, investigations of lossy fibers beyond the weak-loss limit were confined to numerical simulations.

We could recently demonstrate [12] that SY can be used to cover lossy fiber by interpreting continuous loss as a sequence of infinitely many infinitesimal localized losses, each of which can be treated by SY. It became clear, among other things, what the mechanism for the eventual death of a soliton is. While that paper concentrated on loss, the total accumulated loss factor (called $\Gamma < 1$) can easily be used to describe gain, by letting $\Gamma > 1$.

Can solitons be amplified without creating radiation in the process? As shown in [13], that is possible in a very special set of conditions: the soliton needs to have a particular chirp, the fiber parameters must vary along the distance to a certain specification (tapering), and there are constraints on the gain mechanism. Here we consider conventional (unchirped) solitons in conventional (nontapered) fibers, without assumptions about the gain mechanism. Then, radiation-free amplification is possible only in the adiabatic limit, a case of little use in practical terms.

In the general case of more-than-vanishing gain, the question naturally and unavoidably arises: if one starts with a weak (nonsolitonic) pulse and boosts its power, can a soliton

be created? Or, alternatively, if one starts with a soliton and amplifies its power, can a second soliton arise?

The answer is straightforward only if one has localized (stepwise) gain acting on an unchirped pulse as this special case can be treated with SY. For chirped pulses and distributed gain the answer is not obvious at all. We point out that clarification of this issue may be relevant to several contexts. In today's fiber links, optical gain is often provided by Raman amplification which is distributed over a long fiber length. Can a soliton, after suffering from some severe perturbation, be restored to obtain solitonic properties again? Or if one considers a fiber laser, if the gain fiber segment is fed with a weak pulse, can a soliton arise? (In the case of a laser, resonator boundary conditions apply; our treatment covers processes in the gain fiber only.)

In the present paper we address the problem of soliton creation from gain, both localized and distributed. Where closed solutions do not exist, we resort to fits of observed behavior, to arrive at statements with some predictive power.

2. Basic Definitions

The Nonlinear Schrödinger Equation (NLSE) in normalized form is [2, 14, 15]

$$i\frac{\partial}{\partial\xi}u+\frac{1}{2}\frac{\partial^2}{\partial\tau^2}u+|u|^2u=0, \tag{1}$$

where ξ is distance, τ is time, and $u = u(\xi,\tau)$ is the amplitude envelope in a comoving frame of reference. Equation (1) describes the propagation of light in optical fibers in the absence of loss and gain, at anomalous dispersion. Its fundamental soliton solution has the form

$$u(\xi,\tau)=\eta\,\mathrm{sech}(\eta\tau)\exp\left(i\frac{\eta^2}{2}\xi\right), \tag{2}$$

when it rests in the center of the frame of reference. η is the scaling parameter that sets both peak amplitude and inverse duration. That η appears in both reflects the soliton's hallmark balance between dispersive and nonlinear effects, a fact that has also been expressed as an "area theorem" [16] that the product of peak amplitude and width—or, alternatively, peak power times width squared—takes a constant value [14, 15, 17]. Frequently the same is expressed using characteristic length scales for dispersion (L_D) and nonlinearity (L_{NL}) [14, 15]; in our dimensionless units they both take the form $L_D = L_{\mathrm{NL}} = \eta^{-2}$. η^2 appears in the phase term indicating a nonlinear phase rotating at a rate proportional to peak power. The soliton energy is $E_{\mathrm{sol}} = 2\eta$.

We will investigate the evolution of a pulse that is initially not a soliton. In its fullest generality the problem would be intractable, and so we make one simplifying assumption: we consider pulses that have sech amplitude envelope and are initially unchirped. To describe nonsolitonic pulses, we break the link between peak amplitude and inverse duration by introducing an amplitude scaling parameter M. As pulse parameters may evolve during propagation, we abbreviate M_ξ for $M(\xi)$. Hence, the initial condition (the launch pulse at $\xi = 0$) is written as

$$u(0,\tau)=M_0\eta\,\mathrm{sech}(\eta\tau)\overset{!}{=}N\eta\,\mathrm{sech}(\eta\tau). \tag{3}$$

On the RHS we use the soliton order N which compares the relative strength of dispersive and nonlinear effects [14, 15]. The integer number closest to N is the soliton count [3]. $M_\xi = N$ if and only if the pulse is chirp-free. As we always consider chirp-free initial conditions, we do not need to make the distinction at the launch point, but during propagation, M_ξ may and will differ from N. For $M_0 = 1$ the soliton is recovered; in the limit $M_0 \to 0$ the propagation is linear, that is, purely dispersive.

In Section 3.2 we will consider pulses launched with $0 < N < 1/2$, motivated by the well-known fact obtained from Inverse Scattering theory [2] that no soliton is formed if $N < 1/2$. Subsequently, in Section 4.2 we will consider pulses launched with $1/2 < N < 3/2$, that is, from the regime, where there is exactly one soliton, to determine whether a second soliton can arise from gain.

If the gain is localized, it follows from SY that the gain enhances the power at least up to the threshold $N_{\mathrm{thr}} = 1/2$ for the first soliton to appear, $N_{\mathrm{thr}} = 3/2$ for the second, and so on. The minimum required gain $\Gamma = E_{\mathrm{out}}/E_{\mathrm{in}}$ for that is $\Gamma = (N_{\mathrm{thr}}/N)^2$. If the gain is not localized but distributed, more of it is required to reach threshold because there are two opposing trends: the pulse energy grows exponentially with distance ξ as $E_p = E_p(0)\exp(\gamma\xi)$ where we introduce a dimensionless gain coefficient $\gamma > 0$. A characteristic dimensionless gain length is $L_\gamma = \gamma^{-1}$. The gain can be represented in (1) by replacing the RHS with $(i\gamma/2)u$. Energy growth brings the pulse closer to the threshold of soliton generation. At the same time, the pulse undergoes dispersive broadening which renders it temporally broader, lets the peak power droop, and—most importantly—creates a chirp. Power boost helps chirp hinder soliton creation. Therefore we must first discuss the formation of chirp in Section 3.1.

3. The Situation without Gain or Loss

3.1. A Note on Chirp. We start with a comment on the linear, purely dispersive limit. The sech shape typical for solitons is mathematically less convenient than a Gaussian: an initially Gaussian pulse, upon dispersion, remains Gaussian everywhere, except for rescaling, but underneath the Gaussian envelope a linear chirp (quadratic phase profile) develops. According to [14] but written in dimensionless units, its evolution is given by

$$u_D(\xi,\tau)=\frac{A}{\sqrt{1-i\eta^2\xi}}\exp\left[-\frac{(\eta\tau)^2}{2(1-i\eta^2\xi)}\right] \tag{4}$$

with arbitrary amplitude A. At center ($\tau = 0$),

$$\begin{aligned}|u_D(\xi,0)|&=\frac{A}{\sqrt[4]{1+\eta^4\xi^2}},\\ \varphi_D(\xi,0)&=-\frac{1}{2}\arctan\left(\eta^2\xi\right).\end{aligned} \tag{5}$$

This is to be compared to an initially sech-shaped pulse which undergoes some shape variations. Pulse wings exhibit some wiggles around $\xi_0 = \pi/2$ (after one soliton period), but asymptotically the shape is not much different from a chirped sech again at least in its central part. Unfortunately, no closed analytic expression is available to write this evolution. We therefore make the simplifying assumption for the linear regime that the pulse envelope never strays far from the sech shape; indeed assume that the shape is constant except for scaling. This forces us to take into account the different spreading rates of the two shapes by introducing a scaling factor κ for the amplitude and phase evolution in the form

$$\begin{aligned} \left|u_D(\xi,0)\right| &= A\frac{1}{\sqrt[4]{1+\kappa\eta^4\xi^2}}, \\ \varphi_D(\xi,0) &= -\frac{1}{2}\arctan\left(\kappa\eta^2\xi\right). \end{aligned} \tag{6}$$

By varying κ for the best match of both evolutions we find $\kappa = 0.42$ [12].

We now proceed by considering a pulse amplitude that is not vanishingly small. Then there is a nonlinear contribution to the pulse evolution. It was observed early on in numerical work [11] that in the anomalous-dispersion regime considered here this contribution always serves to reduce the broadening. Here, however, we need to evaluate the chirp.

The effect of chirp on the soliton content of a pulse has been studied before. In 1979 Hmurcik and Kaup [16] started from the observation that the McCall-Hahn area theorem in self-induced transparency only applies to unchirped pulses and found that chirped pulses need to be stronger in order to generate the same effect. Desem and Chu [18] 1986 specifically talked about fiber-optic solitons, considered ZS soliton eigenvalues, and found how for (in current usage of terminology) different soliton orders N the power going into the soliton is diminished when chirp is introduced, to the point that a soliton vanishes at some particular value of the chirp, beyond which all power goes into radiation (the soliton order is closely related to the area theorem). Also in 1986, Blow and Wood [19] pursued the relation between the solitonic energy eigenvalue and the pulse's bandwidth. In 1987, Mamistov and Sklyarov [20] determined threshold values of phase modulation beyond which the soliton count in a pulse would be reduced. Kaup et al. [21] 1994 introduced a simplified pulse shape (rectangular amplitude profile, piecewise-linear antisymmetric phase profile) which allowed getting further insight. They found that, for different soliton orders, at the point where the soliton vanishes the phase slope was always close to a characteristic value.

In all cases the results indicate that comparing an unchirped with a chirped pulse of the same energy, a lesser fraction of energy is available for soliton formation in the chirped case. This will become apparent in detail below.

3.2. Evolution of an $N < 1/2$ sech Pulse. Chirp is detrimental to soliton formation; energy gain is conducive to it. With energy growing exponentially with distance and the chirp growing at a much lesser rate (this will be detailed in Figure 3), there will always be a crossover point where the advantage from gain outweighs the disadvantage from chirp. The smaller the gain factor, the longer the distance over which the chirp can develop. Our discussion will thus concentrate on the run-up distance to soliton formation, that is, the position in the amplifying fiber ξ_B where a soliton is created.

The propagation of a "weak" pulse in this framework is fully described by just three parameters: amplitude scaling factor M_ξ, soliton scaling parameter $\eta(\xi) = \eta_\xi$, and chirp coefficient $C(\xi) = C_\xi$. The latter is defined as

$$C = -\left.\frac{\partial^2\varphi(\tau)}{\partial\tau^2}\right|_{\tau=0}, \tag{7}$$

where $\varphi(\tau)$ is the optical phase. A chirped sech pulse at position ξ is then written as

$$u_\xi(\tau) = M_\xi\eta_\xi\,\mathrm{sech}\left(\eta_\xi\tau\right)\exp\left(-i\frac{C_\xi}{2}\tau^2\right). \tag{8}$$

We now follow the evolution of such pulse. It will broaden with distance due to dispersion, but depending on N the nonlinear Kerr effect will counteract and slow down the broadening [11]. Due to energy conservation, the peak amplitude $\eta_\xi M_\xi$ will droop accordingly.

In the linear limit, by way of our approximation, the amplitude evolution is well described [12] by

$$\left|u(\xi,0)\right| = \frac{\eta N}{\sqrt[4]{1+\kappa\left(\eta^2\xi\right)^2}} \tag{9}$$

with a small amplitude factor in the numerator. In the denominator, the relevant variable is $\eta^2\xi$ because the relevant length scales L_{NL} and L_D both scale as η^{-2}. To find a useful expression for the evolution for amplitudes larger than in the linear limit we numerically checked how $|u|$ scales with N and find that

$$\left|u(\xi,0)\right| = \frac{\eta N}{\sqrt[4]{1+\kappa\left(\eta^2\xi\right)^{(2-N^2)}}} \tag{10}$$

makes a very good fit. Data in Figure 1 test this assertion for $\eta = 1$ and several values of N; we have also checked for different η values (not shown). A comparison is shown between plots of (10) (solid curves) and a full numerical simulation which provides a quite accurate reference (dashed curves). The agreement is convincing, confirming that our approximations are quite reasonable.

Energy conservation ensures that

$$2\eta N^2 = 2\eta_\xi M_\xi^2, \tag{11}$$

and the peak amplitude evolves as

$$\left|u(\xi,0)\right| = \eta_\xi M_\xi. \tag{12}$$

Combining (10), (11), and (12) we have

$$M_\xi = N\sqrt[4]{1+\kappa\left(\eta^2\xi\right)^{(2-N^2)}}, \tag{13}$$

$$\eta_\xi = \left(\frac{N}{M_\xi}\right)^2\eta. \tag{14}$$

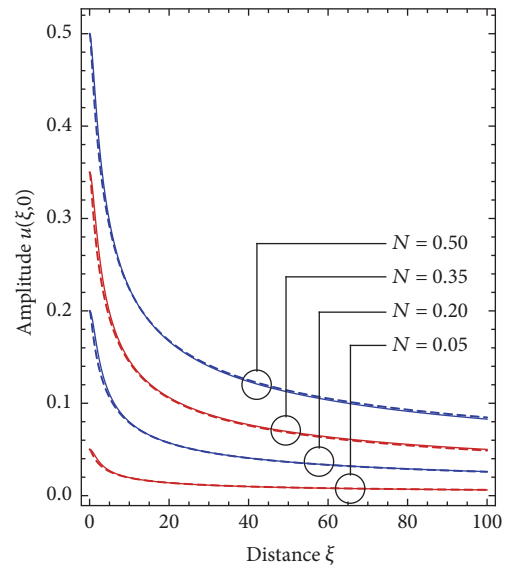

FIGURE 1: Amplitude evolution of weak sech pulses ($N = 0.05$, 0.2, 0.35, and 0.5, as indicated) with $\eta = 1$. Dashed curves: numerical data; solid curves: predictions from (10).

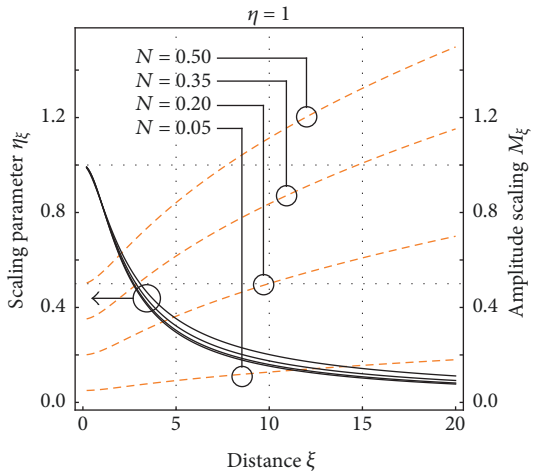

FIGURE 2: Evolution of amplitude scaling factor M_ξ (orange, dashed curves) and scaling parameter η_ξ (black solid curves) with distance, for $N = 0.05$, 0.2, 0.35 and 0.5, as indicated.

In Figure 2, (13) and (14) are plotted for $\eta = 1$ and for $N = 0.05, \ldots, 0.5$. In all cases η_ξ falls with distance (reflecting the broadening), while M_ξ grows. One might suspect that with growing M_ξ a soliton might be created once threshold is reached at $M_\xi = 1/2$. However, that is evidently not the case because the number of solitons, here zero, is guaranteed to be preserved. The discussion is only complete with consideration of the chirp, and it is the development of a chirp that counteracts soliton creation.

We concentrate on the central part of the pulse (between the 80% amplitude points) where the phase is very nearly parabolic. From numerical propagation simulation data we obtain C_ξ by least-squares fit. We let the chirp coefficient $C(0, N, \eta) = 0$ at launch for all N, η. As the pulse propagates, C rises linearly, peaks, and then rolls down as $C(\xi) \propto 1/\xi$ when for $\xi \to \infty$ the pulse duration diverges. By systematic variation of both η and N we determined an expression capturing dependencies on these parameters. The expected inversion symmetry $C(\xi) = -C(-\xi)$ is also built in. This results in

$$C(\xi, N, \eta) = \frac{a\eta^2\left(1 - N^2/4\right)}{\eta^2|\xi| + b(1 + N/2) + 1/\left(\eta^2|\xi|\right)} \operatorname{sgn}(\xi) \quad (15)$$

with fit parameters $a = 1.07$ and $b = 1.40$. Figure 3 shows plots of (15) (solid curves), in comparison to numerical data (dotted). It is clear that (15) is a good approximation over the range of interest, that is, $0 \le N \le 0.5$ and $0.5 \le \eta \le 1.5$. One observation to be made is that, during its dispersive propagation, a weak sech pulse with $\eta = 1$ will never exceed $C \approx 0.4$ which is quite moderate. The other is that chirp values are highest for $N \to 0$: nonlinearity not only slows broadening as asserted in [11], but also reduces chirp.

3.3. Soliton Content of Chirped sech-Shaped Pulses. We are now positioned to determine the soliton content of the pulse under consideration. It is well known [2, 3, 15] that an unchirped sech pulse with $1/2 < N < 3/2$ has pulse energy $E_p = 2\eta N^2$ and contains exactly one soliton with energy $E_{\text{sol}} = 2\eta(2N - 1)$; the balance is radiation with energy $E_{\text{rad}} = 2\eta(N - 1)^2$. We employed the Direct Scattering Transform (DST) technique [22–24] to obtain solitonic eigenvalues from pulses as in (8). Results for various chirp values are shown in Figure 4 as data points. We are not concerned here with the real part of the eigenvalue as all velocities are zero; the imaginary part μ represents the energy of the pertaining solitons, $E_{\text{sol}} = 4\mu$.

This figure is similar to Figure 1 in [18] (with $\phi = C/2$) and to Figure 1 in [25] (with $\phi_0 = C/2$). It shows that the power contained in a chirped pulse can only partially be converted into a soliton: the more the chirp, the lower the soliton energy. For any N there is a "critical" chirp C_{crit} beyond which soliton formation is not possible.

At $C = 0$ all traces start at the well-known value

$$\mu(C = 0, N, \eta) = \left(N - \frac{1}{2}\right)\eta = \mu_0 \quad (16)$$

and then roll down. Different from [25] we observe that this occurs first quadratically, but beyond the diagonal auxiliary line, linearly. In the quadratic regime, an ansatz

$$\mu(C, \mu_0, \eta) = -\frac{C^2}{8\eta^2\mu_0} + \mu_0 \quad (17)$$

fits well, and the same is true for

$$\mu(C, \mu_0, \eta) = -\frac{C}{2.5\eta} + 1.335\,\mu_0 \quad (18)$$

in the linear regime; the crossover occurs at

$$\mu_\chi = \frac{C}{2.5\,\eta}. \quad (19)$$

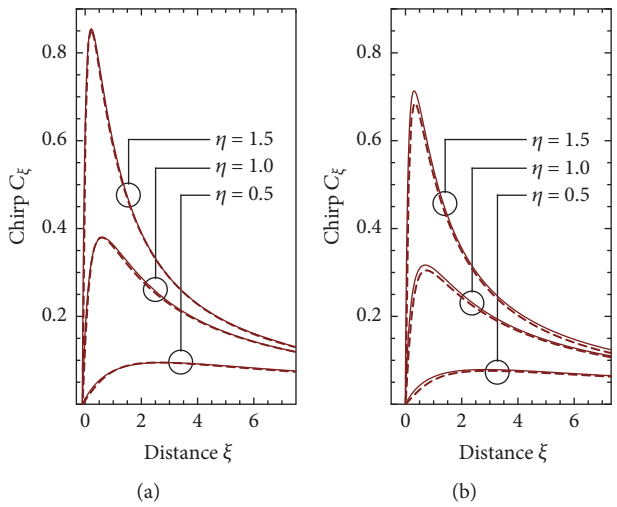

FIGURE 3: Chirp evolution for $\eta = 0.5$ (bottom trace) to $\eta = 1.5$ (top trace) in increments of 0.5. Solid curves represent the approximation (15); dashed curves are numerical data. (a) $N = 0.001$ approximates linear propagation. (b) $N = 0.5$ represents the most extreme case considered here.

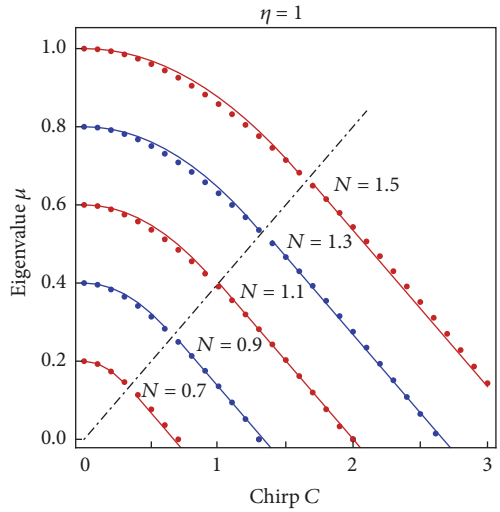

FIGURE 4: Soliton energy eigenvalues when the chirp is varied. Data shown as dots for $\eta = 1$ and $N = 0.7$ (lowest trace); 0.9; 1.1; 1.3; and 1.5 (top trace). Lines: fits with (17) and (18).

Using these fits, the critical chirp value (at $\mu = 0$) is

$$C_{\text{crit}} = 3.34\,\eta^2\left(N - \frac{1}{2}\right). \tag{20}$$

This result coincides with (20) in [25] (their numerical prefactor was 3.28 which agrees within numerical precision); we remark that our two-part function (17) and (18) fits the data, including those in [25], significantly better than the fit given there.

We convinced ourselves that our fit functions hold well for all combinations of $0.5 \le N \le 1.5$ and $0.1 \le \eta \le 10$. As an example we specify for the fundamental soliton with standard values $\eta = 1$, $N = 1$ (the reference soliton): it disappears at $C_{\text{crit}} = 1.67$, and at the crossover point its chirp amounts to $C_\chi = C_{\text{crit}}/2$.

4. Amplified Propagation

We will consider gain in its simplest form, that is, as multiplication of amplitude with a certain gain factor, but without complications like gain saturation, frequency-dependent (selective) gain, and so on. In a purely linear system, it is immaterial whether gain acts at the beginning or at the end of the propagation or is distributed over the distance: both dispersion and gain are linear processes, and they commute. As soon as there are nonlinear phase shifts (or other consequences of nonlinearity), it makes a great difference whether gain is localized or distributed (for the analogous case of loss this was demonstrated in [12]).

4.1. Starting from Pure Radiation. For weak pulses, that is, pulses with powers below the threshold of soliton generation or just at the threshold at most ($0 < N < 1/2$), we may approximate that gain acts only on the amplitude scaling factor M_ξ, without immediate impact on pulse width, chirp, or other shape characteristics. We start by discussing limiting cases.

High Gain ($\gamma \to \infty$). If amplification is applied more or less stepwise before dispersive spreading has set on, the problem is a straightforward application of [3]: all that is required to generate a soliton is to boost M_ξ at least to the threshold value of $M_\xi = N = 1/2$, that is, $\Gamma = 1/(2N)$.

$$M_\xi = N\exp\left(\frac{\gamma}{2}\xi\right) \longrightarrow \xi = \ln\left(\frac{M_\xi^2}{N^2}\right)L_\gamma. \tag{21}$$

For example, starting from an unchirped sech pulse with $N = 0.4$, a first soliton arises at $\xi_B = 0.4463L_\gamma$. (The threshold

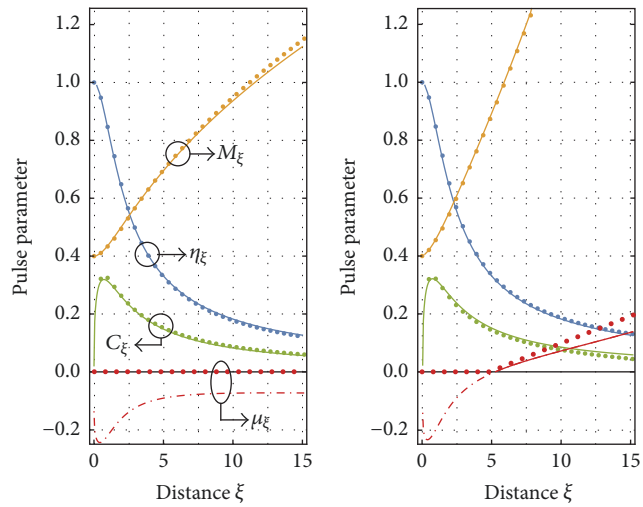

FIGURE 5: Impact of gain: evolution of amplitude scaling parameter M_ξ (orange), scaling parameter η_ξ (blue), chirp C_ξ (green), and soliton content μ_ξ (red) as calculated here (solid/dash-dotted lines) in comparison to numerical simulation (dots). (a) For the integrable NLSE system with $\gamma = 0$ and (b) with gain ($\gamma = 0.1$), soliton appears at $\xi_B \approx 5$. Initial parameters: $N = 0.4$, $\eta = 1$, and $C = 0$.

for a second soliton would be at $M_\xi = 3/2$ and in the same example would be reached at $\xi_B = 2.644 L_\gamma$.) Incidentally, a pure soliton is obtained when the gain lifts M_ξ to 1. If amplification occurs only after some spreading and chirp has developed, the quoted distance is a lower bound.

Adiabatic Gain ($\gamma \to 0$). The signature of the adiabatic case is that the gain length is very much longer than the characteristic dispersion length, so that $L_D/L_\gamma \to 0$. In this limit, no soliton is generated; all of the energy remains in the radiation. We conclude that a soliton count of zero is maintained during adiabatic gain: no soliton will be generated, ever.

Finite Gain. We introduce a gain term into (13),

$$M_\xi = N \sqrt[4]{1 + \kappa \left(\eta^2 \xi\right)^{(2-N^2)}} \exp\left(\frac{\gamma}{2}\xi\right), \tag{22}$$

with gain parameter $\gamma > 0$; it is also possible to let $\gamma < 0$ in which case γ is Beer's coefficient of absorption. The chirp coefficient C_ξ and scaling parameter η_ξ at position ξ can be calculated using the initial values of N and η from (15) and

$$\eta_\xi = \frac{\eta}{\sqrt{1 + \kappa \left(\eta^2 \xi\right)^{(2-N^2)}}}. \tag{23}$$

The eigenvalue component representing the solitonic energy μ_ξ can be obtained from the calculated local values given by (17) and (18).

$$\mu_\xi = -\frac{C_\xi^2}{8\eta_\xi^3\left(M_\xi - 1/2\right)} + \left(M_\xi - \frac{1}{2}\right)\eta_\xi \quad \text{if } C_\xi < 1.67\,\eta_\xi^2\left(M_\xi - \frac{1}{2}\right),$$

$$= -\frac{C_\xi}{2.5\eta_\xi} + 1.335\left(M_\xi - \frac{1}{2}\right)\eta_\xi \quad \text{if } C_\xi > 1.67\,\eta_\xi^2\left(M_\xi - \frac{1}{2}\right). \tag{24}$$

In Figure 5(a) the evolution as predicted by this approximation is shown for the integrable NLSE system with $\gamma = 0$ and at $N = 0.4$. Parameters M_ξ (solid orange line), η_ξ (solid blue line), C_ξ (solid green line), and μ_ξ (dash-dotted red line) are shown. In comparison, corresponding simulation results are shown as dots with matching color. Note that formally the "soliton content" μ_ξ comes out negative when there is no soliton present, while numerics always correctly yields a zero in such case. Theoretical predictions and simulations agree well.

Figure 5(b) shows the same situation as in Figure 5(a) but with a gain of $\gamma = 0.1$. The soliton content μ_ξ is shown as solid red curve for meaningful positive values predicting the existence of a soliton. After a certain distance $\xi_B \approx 5$ the soliton content becomes positive, indicative of the birth of a soliton. This demonstrates that with our formalism the location of the birth of a soliton can be predicted. The slight difference between the predicted positive soliton content and numerical data for ξ well above the threshold arises from the increasing deviation of the numerical pulse from a pure hyperbolic secant shape.

The position of the soliton's birth, ξ_B, is obtained by letting $\mu_\xi = 0$ in (24) and inserting (15), (22), and (23); we do not spell out the resulting rather unwieldy expression here. ξ_B depends on γ and N: large values of either render it short. Predictions of $\xi_B(N, \gamma)$ are shown in Figure 6 as solid curves; numerical results from DST are also shown (dots). It is obvious that the general trends are represented well, but there is a tendency that our equations find ξ_B systematically high.

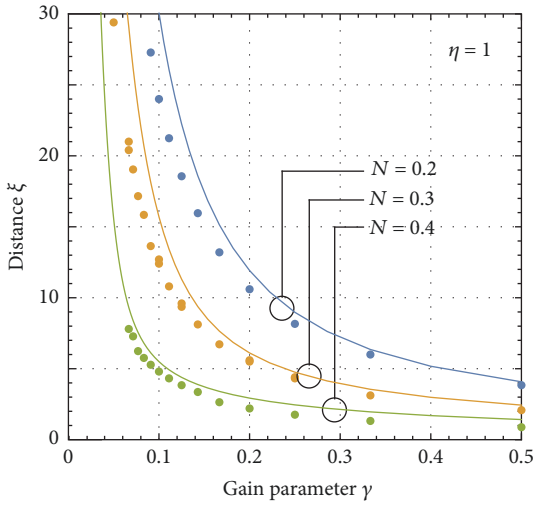

FIGURE 6: The distance until a first soliton appears (ξ_B) depends on the gain factor γ. Shown for $N = 0.2$ (top trace) to $N = 0.4$ (bottom trace) in increments. Solid, predictions; dots, numerical results.

This is particularly true for long distances, surely because then pulse shape differences can play out more. Nevertheless, the agreement with numerics is still good enough for predictions to be useful.

4.2. Starting from One Soliton Plus Radiation. After discussing how gain can bring a weak ($N < 1/2$, "subsolitonic") pulse up to the solitonic threshold, we now consider initial conditions $1/2 < N < 3/2$ so that we start from a pulse which contains both one soliton and some nonsolitonic radiation. The energy E_{rad} of the latter is given by the difference of the pulse energy E_p and the soliton energy E_{sol} [3, 12]:

$$E_{\text{rad}}(0) = 2\eta N^2 - 2\eta(2N-1) = 2\eta(N-1)^2. \quad (25)$$

During amplified propagation,

$$E_{\text{rad}}(\xi) = 2\eta_\xi M_\xi^2 - 4\mu_\xi. \quad (26)$$

A new (second) soliton will always be created from the radiative part once its energy reaches a threshold, as discussed in the previous section. Note that the radiation has two contributions: (i) from the initial condition as in (25) [3, 12], except when $N = 1$; (ii) from continuous generation during amplified propagation, except in the adiabatic limit [12]. This is a consequence of the continuous perturbation of the soliton's characteristic balance between nonlinearity and dispersion.

The main difference to the case of loss as discussed in [12] is that during its propagation the situation becomes more and more diabatic in the lossy fiber, but approaches adiabaticity in the amplifying fiber. This is because in the case of gain the scaling parameter η_ξ grows so that the ratio L_D/L_γ decreases. As shown in [12], the rate of generation of radiative energy is proportional to that ratio. As a result, the radiative fraction of the pulse energy saturates within a few dispersion lengths. For the $N = 1$ soliton we find that it approaches

$$\frac{E_{\text{rad}}(\xi)}{E_p(\xi)} \approx \left(\frac{L_D(0)}{L_\gamma}\right)^2 = \left(\frac{\gamma}{\eta^2}\right)^2. \quad (27)$$

The situation is compounded by the fact that both contributions to radiation and also the soliton are subject to gain all the time. We will again discuss limiting cases first.

High Gain ($\gamma > \eta^2$). Then $L_\gamma < L_D$; in the limit $\gamma \to \infty$ we approach the case of stepwise gain as in SY. No significant change of η_ξ and C_ξ can occur over L_γ; only M_ξ is raised. Then, the second soliton arises once $M_\xi = 3/2$. Using (21) we can predict for the above example of an initially unchirped $N = 0.6$ sech pulse that for $\gamma \to \infty$ the second soliton appears at $\xi_B = 1.833\, L_\gamma$.

Adiabatic Gain ($\gamma \to 0$). In the limit, the soliton does not shed energy to radiation. Thus, both soliton and radiation energy grow exponentially, without redistribution among them. Also, their temporal overlap is minimal because $L_D \ll L_\gamma$, and radiation is rapidly broadened. In consequence, even after a vast propagation distance no further solitons will arise (i.e., $\xi_B \to \infty$).

Small Gain ($\gamma < \eta^2$). The equilibrium between nonlinearity and dispersion is approximately maintained because the soliton can rearrange its width and peak power at a rate that nearly keeps up with the change. Therefore, if there is any sizable amount of radiative energy from the initial condition, it will dominate.

In [12] we derived an expression for the amplitude evolution of a sech pulse in the presence of initial radiation. Here an extended version in dimensionless form is given including the impact of distributed gain depending on γ.

$$|u(\xi,0)| = \eta \exp(\gamma\xi)\left[(2N-1) + \frac{1-N}{\sqrt[4]{1+\kappa(\eta^2\xi)^2}}\right.$$
$$\times \cos\left\{\frac{(2N-1)^2\eta^2}{2}\exp\left(\gamma\xi^{1+\epsilon}\right)\xi\right. \quad (28)$$
$$\left.\left. + \frac{1}{2}\arctan\left(\kappa\eta^2\xi\right)\right\}\right].$$

The first term on the RHS is the exponentially growing amplitude, under the assumption that the sech shape is basically preserved, and taking the pulse narrowing into account. Inside the square bracket, the first parenthesis pertains to the initial soliton. The prefactor of the cosine term models the dispersive broadening. The argument of the cosine contains one term for the nonlinear phase rotation and one for the Guoy shift [12]; both together define the beating between soliton and radiation. Incidentally, we find empirically that the nonlinear phase, which follows the peak amplitude, is modelled slightly better with a correction $\epsilon = 0.03$

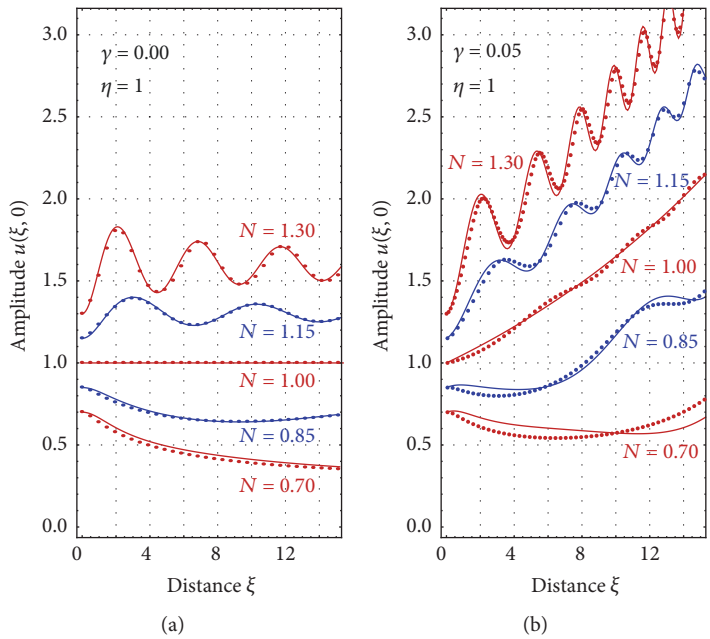

FIGURE 7: (a) Evolution of pulse amplitude from model (solid curve) and numerics (dots) for initial values of $N = 0.7, \ldots, 1.3$. (b) Same propagation with included gain ($\gamma = 0.05$, $\epsilon = 0.03$).

as indicated, apparently because the sech shape is not strictly preserved.

We put (28) to a numerical test. We considered the propagation of an initially $1/2 < N < 3/2$ sech pulse, first without gain by setting $\gamma = 0$. This is shown in Figure 7(a) for values of $N = 0.7, \ldots, 1.3$. Again solid curves (dots) correspond to theoretical prediction (numerical data), respectively. Pulse parameters oscillation due to beating of the solitonic and dispersive part of the pulse. Incidentally, this figure closely resembles Figure 2 in SY [3], but they only had numerical data. Here the agreement between numerical data and (28) is very good. The oscillation frequency is constant because in the absence of gain the nonlinear phase rotates at a constant rate.

In contrast, Figure 7(b) shows similar data but with weak gain ($\gamma = 0.05$). As the amplitude builds up (on average), the oscillation frequency also increases. Again numerics and theory agree well.

From the amplitude the pulse parameters M_ξ and η_ξ can be calculated using

$$M_\xi = \frac{\eta N^2 \exp(\gamma\xi)}{|u(\xi, 0)|}, \qquad \eta_\xi = \left(\frac{N}{M_\xi}\right)^2 \exp(\gamma\xi)\,\eta. \tag{29}$$

In Figure 8 the parameter evolution for an initially unchirped $N = 1.2$ sech pulse is shown for $\gamma = 0$ (constant energy; (a)) and $\gamma = 0.05$ (gain; (b)).

M_ξ and η_ξ agree well with numerics. The chirp parameter C is here only obtained from numerics. It is obvious that the chirp oscillates around zero with moderate values resulting in only a slight change of the soliton content. Thus for the calculation of the soliton content the chirp was neglected resulting in the simple expression

$$\mu_\xi = \eta_\xi \left(M_\xi - \frac{1}{2}\right). \tag{30}$$

The soliton eigenvalue is shown in red in Figure 8: predictions of (30) (solid) and numerical results (dotted) are compared and show good agreement. The gain causes the scaling factor η_ξ to rise, but not the amplitude scaling factor M_ξ which undulates around unity and represents a fundamental soliton.

4.3. Generation of a Second Soliton. So far we discussed the evolution of the first soliton; now we turn to a discussion of the second soliton. We traced the energy partition between solitons and radiation by evaluating the nonlinear spectrum. For Figure 9 an unchirped sech pulse ($\eta = 1$, $N = 1.3$) was launched into a fiber with $\gamma = 0.1$ and propagated numerically up to $\xi = 10.0$. Undulations indicate beating between constituents, and there may be some amount of energy swapping. That notwithstanding so much is clear: both soliton 1 and radiation grow from their initial value up to the onset of soliton 2 at $\xi_B = 8$ (arrow); beyond that point the radiative energy drops. The second soliton is clearly created from radiation energy, without depletion of the first soliton.

As an example of an actual pulse shape we show the field envelope at $\xi = 9.32$ (Figure 9(b)). The pulse shape consists of a narrow, tall peak atop a broad, low-amplitude pedestal. One can fit a sech pulse with $M_\xi = 0.965$ and $\eta_\xi = 4.43$ with flat phase to the narrow spike, and $M_\xi = 1.22$ and $\eta_\xi = 0.185$ with parabolic phase ($C = 0.076$) to the pedestal. Using (18) and (30) this suggests eigenvalues of $\mu_1 = 2.06$ (narrow peak) and $\mu_2 = 0.014$ (pedestal). DST analysis yields $\mu_1 = 2.024$ and

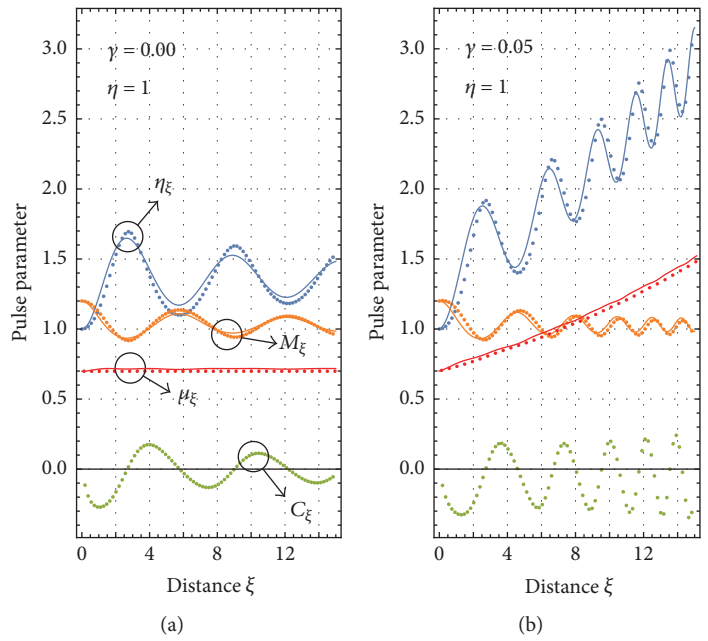

FIGURE 8: Parameter evolution and soliton content (red) of an initial unchirped $N = 1.2$ sech pulse in the case without gain (a) and with gain (b). Again solid curves/dots correspond to the model/numerics, respectively.

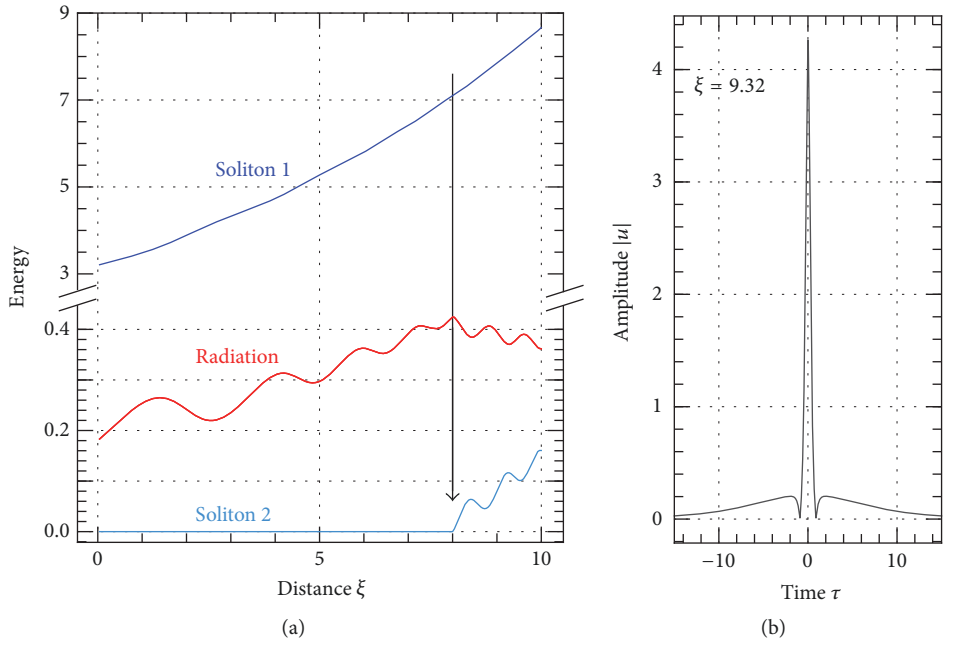

FIGURE 9: (a) Evolution of the energies of both solitons and radiation at $\gamma = 0.1$, calculated from Direct Scattering Transform. Initial conditions were $N = 1.3$ and $\eta = 1.0$. Note the break in the scale. The point of creation of the second soliton is highlighted by an arrow. (b) Example of a pulse envelope taken at $\xi = 9.32$ where the pulse consists of two solitons and radiation.

$\mu_2 = 0.029$, respectively. In view of approximations made, the agreement is reassuring. One is led to conclude that the high peak almost exclusively represents the higher-energy soliton, while the second soliton and radiation together form the pedestal. Such identification is possible and meaningful because there is a large difference in solitonic energies (almost two orders of magnitude); the resulting different widths lead to minimal temporal overlap.

In Figure 10 we assess the whole range of γ values numerically for four values of N. Arrows on the right mark the predicted emergence length obtained from (21) for high values of γ.

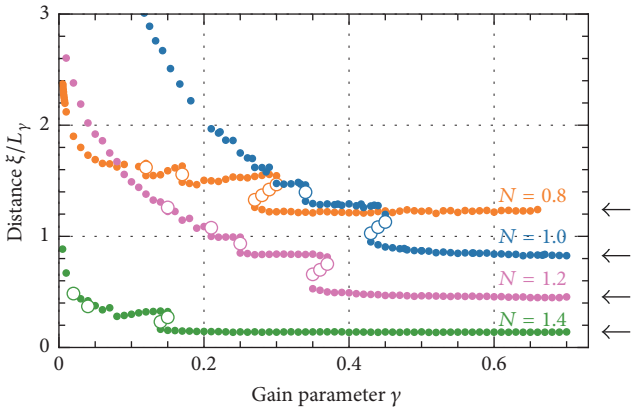

FIGURE 10: Position of creation of the second soliton (dots) as a function of gain parameter γ, for several initial soliton orders N. Open circles: disappearance of the second soliton; see text. Distance is normalized to $L_\gamma = 1/\gamma$. Arrows mark distances as predicted by (21).

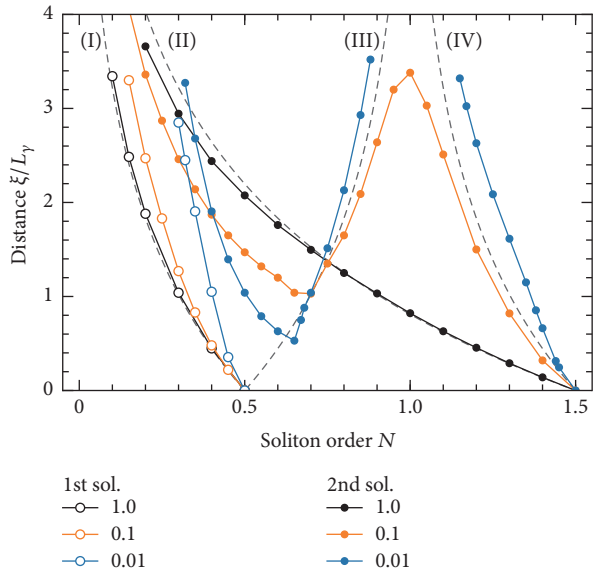

FIGURE 11: Propagation distance until a new soliton is generated. Distance is normalized to L_γ; therefore, values also represent the accumulated gain up to that point. Parameter: γ as indicated. For reference, auxiliary lines (I–IV) indicate certain limiting cases; see text.

Solitons arise from the radiative energy once there is "enough of it." This implies that, beginning at the point of soliton creation, radiative energy is depleted; usually the depletion rate is initially faster than the restoration rate by gain. This is in fact visible in all calculations. Indeed, the partition of energy between radiation and soliton has some oscillation with the beat frequency as seen in Figure 9. We note that the new soliton arises near a radiation maximum in the oscillation cycle. Indeed, this can go so far that the subsequent downswing of the oscillation, combined with the depletion, can cause such a rapid sagging of radiative energy that it falls below the threshold again. In such case the just-created soliton disappears again and returns during the next cycle of oscillations. Accordingly the energy of the emerged second soliton does not rise monotonically but in an oscillating manner. Such on-and-off soliton creation appears in Figure 10 as a folding over of the curves; note the open circles for the reverse branches. Arrows mark distances as predicted by (21).

The normalized position of first and second soliton generation is shown in an overview in Figure 11. Note that position $\xi/L_\gamma = \xi\gamma$ so that it also represents the total accumulated amplification $\ln(\Gamma)$. We inserted auxiliary lines to indicate the limiting cases in which the radiation from the initial condition is amplified in a single step. Line (I) applies to the creation of the first soliton (see (21) with $M_\xi = 1/2$); it diverges at $N \to 0$ for lack of power. Similarly, (II) is for the creation of two solitons at once at $M_\xi = 3/2$; this curve also diverges at $N = 0$ and continues to $N = 3/2$. Data are shown for several values of γ. They show the onset of the first soliton to be above (I) by a difference that grows with decreasing γ. This is expected because lower gain necessitates a longer distance to accumulate the same amplification, but then dispersion will develop more chirps. The onset of two solitons near (II) occurs below the curve because solitons generated from chirped pulse take lower energy values; thus, the first soliton does not fully deplete the radiative energy.

Lines (III) and (IV) appear in the realm where the initial condition contains one soliton plus some radiation, that is, for $1/2 < N < 3/2$, with the exception of $N = 1$, where the initial condition does not contain radiation. Note that (IV) is a shifted version of (I), and (III) is a mirrored version thereof. These curves refer to the situation where a second soliton is formed from the radiative part. This assumes relatively independent evolution of soliton and radiation, justified for small gain ($\gamma \ll 1$) because dispersion broadens the radiative part rapidly so that the mutual overlap is minimal. Therefore, data are closer to (III) and (IV) when the gain is low, while for high gain, data tend towards (II) as expected. There is an interesting transition between both limiting cases, where near $N = 1$ where the initial condition has no radiation; the radiation generated during propagation becomes dominant.

5. Conclusion

It is well known from SY [3] that if one considers an unchirped sech pulse of certain width and scales up its energy, above some threshold it contains a soliton, and above certain higher thresholds more solitons appear. The thresholds are given by the amount of radiative energy.

We were curious to see how this translates into the case of an optical fiber with gain. That situation is more complex because (i) chirp develops during propagation, and (ii) radiation can come from two different sources: the initial condition and the generation during amplified propagation. These circumstances render it less than obvious whether gain leads to the creation of solitons.

By writing an expression for the chirp and by tracking the energy budget, we determined the distance for a new

soliton to appear. We verified that the soliton is formed from radiative energy; if another soliton is already present, its energy is not depleted. As long as the fiber length exceeds the creation distance, a soliton will be created under almost all circumstances, the sole exception being the limiting case of adiabatic amplification where the creation distance diverges. As prior investigations treated the problem within the adiabatic approximation, predictions as given here have not been possible before.

In any realistic setting, solitonic data transmission will incorporate both loss and gain in the fiber. In the design of such systems it is mandatory to understand the impact of those factors well, and not just in the somewhat unrealistic adiabatic limit. Our results may also be of interest for investigations of amplification in a fiber laser when the formation of solitonic pulses is desired.

Conflicts of Interest

The authors declare that there are no conflicts of interest regarding the publication of this paper.

References

[1] W. Forysiak, "Dispersion managed solitons and real-world link installation," in *Proceedings of the 2003 IEEE LEOS Annual Meeting Conference Proceedings*, p. 842, usa, October 2003.

[2] V. E. Zakharov and A. B. Shabat, "Exact Theory of Two-Dimensional Self-Focusing and One-Dimensional Self-Modulation of Waves in Nonlinear Media," *Soviet Physics—JETP*, vol. 34, pp. 62–69, 1972.

[3] J. Satsuma and N. Yajima, "Initial value problems of one-dimensional self-modulation of nonlinear waves in dispersive media," *Progress of Theoretical and Experimental Physics*, pp. 284–306, 1974.

[4] A. Hasegawa and F. Tappert, "Transmission of stationary nonlinear optical pulses in dispersive dielectric fibers. I. Anomalous dispersion," *Applied Physics Letters*, vol. 23, no. 3, pp. 142–144, 1973.

[5] L. F. Mollenauer, R. H. Stolen, and J. P. Gordon, "Experimental observation of picosecond pulse narrowing and solitons in optical fibers," *Physical Review Letters*, vol. 45, no. 13, pp. 1095–1098, 1980.

[6] A. Hasegawa and Y. Kodama, "Signal Transmission by Optical Solitons in Monomode Fiber," *Proceedings of the IEEE*, vol. 69, no. 9, pp. 1145–1150, 1981.

[7] D. J. Kaup, "A perturbation expansion for the Zakharov-Shabat inverse scattering transform," *SIAM Journal on Applied Mathematics*, vol. 31, no. 1, pp. 121–133, 1976.

[8] V. I. Karpman and E. M. Maslov, "Perturbation theory for solitons," *Soviet Physics—JETP*, vol. 73, no. 2, pp. 281–291, 1977.

[9] Y. Kodama and A. Hasegawa, "Amplification and reshaping of optical solitons in glass fiber-II," *Optics Expresss*, vol. 7, no. 7, pp. 339–341, 1982.

[10] K. J. Blow and N. J. Doran, "High bit rate communication systems using non-linear effects," *Optics Communications*, vol. 42, no. 6, pp. 403–406, 1982.

[11] K. J. Blow and N. J. Doran, "The asymptotic dispersion of soliton pulses in lossy fibres," *Optics Communications*, vol. 52, no. 5, pp. 367–370, 1985.

[12] F. Mitschke, A. Hause, and C. Mahnke, "Solitons in fibers with loss beyond small perturbation," *Physical Review A: Atomic, Molecular and Optical Physics*, vol. 96, no. 1, Article ID 013826, 2017.

[13] G. M. Melchor, M. A. Granados, and G. H. Corro, "On the problem of ideal amplification of optical solitons," *Quantum Electronics*, vol. 32, no. 11, pp. 1020–1028, 2002.

[14] G. P. Agrawal, *Nonlinear Fiber Optics*, Academic Press, Waltham, Mass, USA, 5th edition, 2013.

[15] F. Mitschke, *Fiber Optics: Physics and Technology*, Springer, Heidelberg, Germany, 2nd edition, 2016.

[16] L. V. Hmurcik and D. J. Kaup, "Solitons created by chirped initial profiles in coherent pulse propagation," *Journal of the Optical Society of America*, vol. 69, no. 4, pp. 597–604, 1979.

[17] L. F. Mollenauer and J. P. Gordon, *Solitons in Optical Fibers: Fundamentals and Applications*, Academic Press, Burlington, Mass, USA, 2006.

[18] C. Desem and P. L. Chu, "Effect of chirping on solution propagation in single-mode optical fibers," *Optics Expresss*, vol. 11, no. 4, pp. 248–250, 1986.

[19] K. J. Blow and D. Wood, "The evolution of solitons from non-transform limited pulses," *Optics Communications*, vol. 58, no. 5, pp. 349–354, 1986.

[20] A. I. Mamistov and Yu. M. Sklyarov, "Influence of regular phase modulation on formation of soliton pulses," *Soviet Journal of Quantum Electronics*, vol. 17, pp. 500–504, 1987.

[21] D. J. Kaup, J. El-Reedy, and B. A. Malomed, "Effect of a chirp on soliton production," *Physical Review E: Statistical, Nonlinear, and Soft Matter Physics*, vol. 50, no. 2, pp. 1635–1637, 1994.

[22] G. Boffetta and A. R. Osborne, "Computation of the direct scattering transform for the nonlinear Schroedinger equation," *Journal of Computational Physics*, vol. 102, no. 2, pp. 252–264, 1992.

[23] M. I. Yousefi and F. R. Kschischang, "Information transmission using the nonlinear Fourier transform, Part II: Numerical methods," *Institute of Electrical and Electronics Engineers Transactions on Information Theory*, vol. 60, no. 7, pp. 4329–4345, 2014.

[24] F. Mitschke, C. Mahnke, and A. Hause, "Soliton content of fiber-optic light pulses," *Applied Sciences (Switzerland)*, vol. 7, no. 6, article no. 635, 2017.

[25] D. Anderson, M. Lisak, and T. Reichel, "Asymptotic propagation properties of pulses in a soliton-based optical-fiber communication system," *Journal of the Optical Society of America B: Optical Physics*, vol. 5, no. 2, pp. 207–210, 1988.